Quantum-Mechanical Relation between Atomic Dipole Polarizability and the van der Waals Radius (Supplemental Material)

Dmitry V. Fedorov,[1] Mainak Sadhukhan,[1] Martin Stöhr,[1] and Alexandre Tkatchenko[1]

[1]*Physics and Materials Science Research Unit,*
University of Luxembourg, L-1511 Luxembourg

Derivation of the repulsive exchange energy within the QDO model

Here, the Heitler-London approach [32] is applied to the quantum Drude oscillator model [23]. For a homonuclear dimer consisting of atoms A and B separated by $\mathbf{R}$, the corresponding atomic QDO wave functions are given by (we use atomic units but keep $\hbar$ explicitly)

$$\Psi_A(\mathbf{r}) = \left(\frac{\mu\omega}{\pi\hbar}\right)^{3/4} e^{-\frac{\mu\omega}{2\hbar}r^2} \quad \text{and} \quad \Psi_B(\mathbf{r}) = \left(\frac{\mu\omega}{\pi\hbar}\right)^{3/4} e^{-\frac{\mu\omega}{2\hbar}(\mathbf{r}-\mathbf{R})^2} \ , \tag{S1}$$

respectively. Here, $\sqrt{\frac{\hbar}{\mu\omega}}$ is the characteristic length of the QDO. The related overlap integral is

$$S = \iint d\mathbf{r}_1 d\mathbf{r}_2 \ \Psi_A^*(\mathbf{r}_1)\Psi_B^*(\mathbf{r}_2)\Psi_B(\mathbf{r}_1)\Psi_A(\mathbf{r}_2) = e^{-\frac{\mu\omega}{2\hbar}R^2} \ . \tag{S2}$$

We use the dipole approximation for the Coulomb interaction

$$\hat{V}_{\text{dip}} = q^2 \left\{ \frac{[\mathbf{r}_1 \cdot (\mathbf{r}_2 - \mathbf{R})]}{R^3} - \frac{3(\mathbf{r}_1 \cdot \mathbf{R})[(\mathbf{r}_2 - \mathbf{R}) \cdot \mathbf{R}]}{R^5} \right\} \ , \tag{S3}$$

where the origin of the coordinates $\mathbf{r}_1$ and $\mathbf{r}_2$ of the two QDOs is located on atom A.

Then, the corresponding Coulomb and exchange integrals are obtained as

$$C = \iint d\mathbf{r}_1 d\mathbf{r}_2 \ \Psi_A^*(\mathbf{r}_1)\Psi_B^*(\mathbf{r}_2)\hat{V}_{\text{dip}}\Psi_A(\mathbf{r}_1)\Psi_B(\mathbf{r}_2) = 0 \tag{S4}$$

and

$$J_{\text{ex}} = \iint d\mathbf{r}_1 d\mathbf{r}_2 \ \Psi_A^*(\mathbf{r}_1)\Psi_B^*(\mathbf{r}_2)\hat{V}_{\text{dip}}\Psi_B(\mathbf{r}_1)\Psi_A(\mathbf{r}_2) = \frac{q^2 S}{2R} \ , \tag{S5}$$

respectively. We assume that the coarse-grained atomic QDO wave functions represent closed electronic shells with total zero spin. According to their bosonic nature, the dimer wave function can only be symmetric (permanent)

$$\Psi(\mathbf{r}_1, \mathbf{r}_2) = \frac{1}{\sqrt{2}} \left[\Psi_A(\mathbf{r}_1)\Psi_B(\mathbf{r}_2) + \Psi_A(\mathbf{r}_2)\Psi_B(\mathbf{r}_1)\right] \tag{S6}$$

with the corresponding energy obtained as

$$E = \frac{\iint d\mathbf{r}_1 d\mathbf{r}_2 \Psi^*(\mathbf{r}_1, \mathbf{r}_2)\hat{H}\Psi(\mathbf{r}_1, \mathbf{r}_2)}{\iint d\mathbf{r}_1 d\mathbf{r}_2 \Psi^*(\mathbf{r}_1, \mathbf{r}_2)\Psi(\mathbf{r}_1, \mathbf{r}_2)} = 2E_0 + \frac{C + J_{\text{ex}}}{1 + S} = 2E_0 + \frac{J_{\text{ex}}}{1 + S} \ , \tag{S7}$$

where

$$\hat{H} = \hat{H}_0(\mathbf{r}_1) + \hat{H}_0(\mathbf{r}_2) + \hat{V}_{\text{dip}}(\mathbf{r}_1, \mathbf{r}_2) \tag{S8}$$

with

$$\hat{H}_0(\mathbf{r})\Psi_A(\mathbf{r}) = E_0\Psi_A(\mathbf{r}) \quad \text{and} \quad \hat{H}_0(\mathbf{r})\Psi_B(\mathbf{r}) = E_0\Psi_B(\mathbf{r}) \ . \tag{S9}$$

At the equilibrium distance, $R = 2R_{\rm vdW}$, of homonuclear dimers consisting of the species of Table I, the condition $S \ll 1$ is fulfilled:

$$
\begin{aligned}
S_{\rm He–He} &= 6.94 \times 10^{-4} \ , \\
S_{\rm Ne–Ne} &= 4.69 \times 10^{-4} \ , \\
S_{\rm Ar–Ar} &= 3.95 \times 10^{-3} \ , \\
S_{\rm Kr–Kr} &= 5.58 \times 10^{-3} \ , \\
S_{\rm Xe–Xe} &= 1.28 \times 10^{-2} \ , \\
S_{\rm Rn–Rn} &= 2.01 \times 10^{-2} \ .
\end{aligned}
$$

Then, neglecting the second and higher order terms with respect to the overlap integral, the repulsive exchange energy can be well approximated by

$$
E_{\rm ex} \approx J_{\rm ex} = \frac{q^2 S}{2R} = \frac{q^2}{2R} \ e^{-\frac{\mu\omega}{2\hbar}R^2} \ . \tag{S10}
$$

The corresponding force is obtained as

$$
F_{\rm ex} = -\nabla_R J_{\rm ex} = \frac{q^2}{2} \left[\frac{\mu\omega}{\hbar} + \frac{1}{R^2} \right] \ e^{-\frac{\mu\omega}{2\hbar}R^2} \ . \tag{S11}
$$

According to Table I, at the equilibrium distance of the homonuclear dimers ($R = 2R_{\rm vdW}$), $\frac{\mu\omega}{\hbar}$ is an order of magnitude larger than $\frac{1}{R^2}$:

$$
\begin{aligned}
\left(\tfrac{\mu\omega}{\hbar}\right)_{\rm He} &= 0.5178 \ , & \left(\tfrac{1}{R^2}\right)_{\rm He–He} &= 0.0356 \ ; \\
\left(\tfrac{\mu\omega}{\hbar}\right)_{\rm Ne} &= 0.4526 \ , & \left(\tfrac{1}{R^2}\right)_{\rm Ne–Ne} &= 0.0295 \ ; \\
\left(\tfrac{\mu\omega}{\hbar}\right)_{\rm Ar} &= 0.2196 \ , & \left(\tfrac{1}{R^2}\right)_{\rm Ar–Ar} &= 0.0198 \ ; \\
\left(\tfrac{\mu\omega}{\hbar}\right)_{\rm Kr} &= 0.1778 \ , & \left(\tfrac{1}{R^2}\right)_{\rm Kr–Kr} &= 0.0171 \ ; \\
\left(\tfrac{\mu\omega}{\hbar}\right)_{\rm Xe} &= 0.1309 \ , & \left(\tfrac{1}{R^2}\right)_{\rm Xe–Xe} &= 0.0150 \ ; \\
\left(\tfrac{\mu\omega}{\hbar}\right)_{\rm Rn} &= 0.1092 \ , & \left(\tfrac{1}{R^2}\right)_{\rm Rn–Rn} &= 0.0140 \ .
\end{aligned}
$$

Therefore, one can use the following approximation

$$
F_{\rm ex} \approx \frac{q^2}{2} \frac{\mu\omega}{\hbar} \ e^{-\frac{\mu\omega}{2\hbar}R^2} = \frac{\alpha\hbar\omega}{2} \left(\frac{\mu\omega}{\hbar}\right)^2 \ e^{-\frac{\mu\omega}{2\hbar}R^2} \ , \tag{S12}
$$

where it is taken into account that the dipole polarizability is given by $\alpha = q^2/\mu\omega^2$ within the QDO model [23], which corresponds to Eq. (3) of the main manuscript.

The performed derivation is not as obvious as the more conventional approach [30] efficiently used for noble gases, which is based on the consideration of each single pair of interacting electrons. Such a detailed treatment is impossible within the coarse-grained QDO model [23], where the wave function of a single oscillator (a Drude particle) represents all valence electrons together. However, taking into account the bosonic nature of closed valence electron shells, our approach is straightforward. The validity of Eqs. (S10) and (S12) is confirmed by the reasonable agreement between the ratio $R_{\rm vdW}/\alpha^{1/7}$ obtained either within the QDO model or with the reference data for real atoms, as demonstrated by Table I.

The theoretical background of the obtained scaling law between the vdW radius and the polarizability was illustrated above by employing the QDO model. Here, we show another way to prove the proportionality $R_{\rm vdW} \propto \alpha^{1/7}$. Let us consider the repulsive interaction in the Born-Mayer form $E_{\rm ex} = Ae^{-bR}$ used in the Tang-Toennies potential [34], which is known to provide accurate description of the van der Waals interaction [35]. The corresponding repulsive force is then obtained as $F_{\rm ex} = Abe^{-bR}$. On the other hand, the general expression for the attractive dipole-dipole dispersion force is given by $F_{\rm disp} = -6C_6/R^7$. From the force balance condition, one can obtain $R_{\rm vdW} = C(A, b, C_6, \alpha, R_{\rm vdW})\,\alpha^{1/7}$. Here, the proportionality function $C = \frac{1}{2}\left(\frac{6C_6}{\alpha A b}\right)^{1/7} \exp\left(\frac{2bR_{\rm vdW}}{7}\right)$ formally depends on the polarizability. However, due to $C_6 \propto \alpha^2$ and the direct proportionality of the exchange repulsive energy to the dipole polarizability [36], this dependence vanishes. Moreover, based on the parameters of Ref. [35] present for some of the noble gases in our Table I, we obtain: $C^{\rm Ar} = 2.29$, $C^{\rm Kr} = 2.32$, and $C^{\rm Xe} = 2.23$. These values are close to the results of the QDO model showing even the same trend: $C^{\rm Ar} = 2.33$, $C^{\rm Kr} = 2.35$, and $C^{\rm Xe} = 2.28$.

Thus, within two different model approaches, the same scaling law with an approximately constant behavior of the proportionality function is obtained. This indicates the existence of a direct connection between the repulsive and attractive parts of the vdW interaction, which is already quite well captured by the models. To completely reveal its physical origin, further fundamental investigations are desirable.

Extended statistical analysis of the reference data

Here, we perform an extended statistical analysis for the six noble gases of Table I, considering the function

$$C(p, \alpha, R_{\rm vdW}) = R_{\rm vdW}^{\rm ref}/(\alpha^{\rm ref})^p \ . \tag{S13}$$

The reference values for the atomic dipole polarizability and the vdW radius are taken from Refs. [12] and [8,19] of the main manuscript, respectively. The following different possible power laws are assumed: $p \in \{1/3; 1/4; 1/5; 1/6; 1/7; 1/8; 1/9; 1/10; 1/100\}$. We calculate the arithmetic mean

$$\langle C \rangle = \frac{1}{6} \sum_{i=1}^{6} C_i \ \ , \tag{S14}$$

the standard deviation

$$\sigma = \left[\frac{1}{(6-1)} \sum_{i=1}^{6} \left(C_i - \langle C \rangle \right)^2 \right]^{1/2} \ \ , \tag{S15}$$

and the coefficient of variation

$$c_v = \frac{\sigma}{\langle C \rangle} \times 100\% \ \ . \tag{S16}$$

The corresponding results are presented in Table S I. Obviously, the relation between the vdW radius and the polarizability given by Eq. (7) is most reasonable among all considered power laws. The related standard deviation of 0.02 is the minimal one and the coefficient of variation is less than 1%. The other assumed relations do not provide such a good statistical picture. We also show (in parentheses of Table S I) the results for all the 72 chemical elements (6 noble gases, hydrogen, and 65 elements of Batsanov [16]) considered in the main manuscript. For the power law of 1/7, the fitted proportionality constant is changed by just 0.4% in comparison to the case of the noble gases only. By contrast, the corresponding changes for 1/6 and 1/8 power laws are 4.2% and 2.7%, respectively. These results corroborate the analytically-derived scaling law from the statistical analysis of the reference data.

TABLE S I: Results of the extended statistical analysis for the noble gases (He, Ne, Ar, Kr, Xe, and Rn). The related values for all the 72 chemical elements considered in the main manuscript are given in parentheses.

p	1/3	1/4	1/5	1/6	**1/7**	1/8	1/9	1/10	1/100
$\langle C \rangle$	1.71 (1.24)	2.02 (1.69)	2.24 (2.03)	2.41 (2.31)	**2.54** (2.53)	2.64 (2.71)	2.73 (2.86)	2.80 (2.99)	3.46 (4.26)
σ	0.44 (0.30)	0.28 (0.23)	0.16 (0.17)	0.07 (0.12)	**0.02** (0.10)	0.07 (0.11)	0.12 (0.13)	0.17 (0.16)	0.58 (0.59)
c_v (in %)	25.51 (24.21)	13.92 (13.74)	7.15 (8.19)	2.75 (5.14)	**0.65** (3.91)	2.75 (4.02)	4.50 (4.69)	5.90 (5.46)	16.85 (13.80)

Dependence of the obtained results on the reference polarizability

In the main manuscript, we used the atomic dipole polarizability from Table A.1 of Ref. [12], as the reference dataset. Here, Fig. S 1 shows the results obtained with α taken from the benchmark "Dataset for All Neutral Atoms" of Ref. [14]. Comparing it to Fig. 2, the mean of the relative error, $\langle$R.E.$\rangle$, and its magnitude, $\langle|$R.E.$|\rangle$, are pratically the same. This is caused by the fact that α is a well-determined quantity [9-14]. A remarkable difference is present only for Pd where R.E. changes from -10.11% to 3.07%. However, as discussed in the main manuscript, the values of $R^{\rm ref}_{\rm vdW}$ for transition metals are not well reliable, to judge which from the two polarizabilities for Pd is more accurate. Moreover, for organic elements corresponding to the most robust values of $R^{\rm ref}_{\rm vdW}$, the agreement with the reference vdW radius becomes slightly worse in comparison to Fig. 2. In addition to Fig. S 1, Table S II provides a more detailed information about the used reference data as well as the results obtained for $R_{\rm vdW}(\alpha)$.

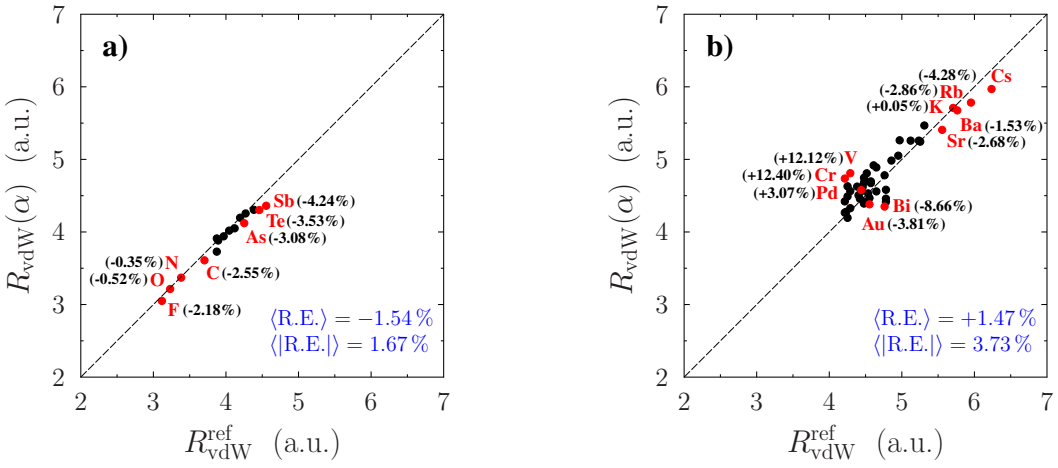

FIG. S 1: (Color online) The vdW radius obtained with Eq. (7) by using the reference data for the polarizability from Ref. [14] is shown separately for a) nonmetals/metalloids and b) metals in comparison to its reference counterpart [15]. Here, $\langle$R.E.$\rangle$ and $\langle|$R.E.$|\rangle$ represent the mean of the relative error and its magnitude, respectively, calculated with Eq. (8) taking $R^{\rm ref}_{\rm vdW}$ from the database of Batsanov [16].

Based on the analysis of the obtained results, we conclude that the choice of the reference dipole polarizability between two available databases plays no role for our conclusions made in the main manuscript.

Equilibrium distance in heteronuclear dimers of noble gases

As complementary to Fig. 3 of the main manuscript, Fig. S 2 and Table S III present more detailed results for the equilibrium distance in vdW-bonded heteronuclear dimers of noble gases obtained with Eqs. (9)–(12). In principle, Eqs. (11) and (12) are equivalent, since

$$2.54\,(\sqrt{\alpha_A \alpha_B})^{1/7} = \sqrt{R^A_{\rm vdW} R^B_{\rm vdW}}\ , \tag{S17}$$

according to Eq. (7). The present tiny differences between the related results are caused by errors in the reference data for the vdW radii and the polarizabilities. In comparison to Eqs. (11) and (12), the results obtained with Eq. (10) are slightly more accurate. Taking into account that Eqs. (10) and (12) are the two approximations often used in literature, we can judge that the approach based on the arithmetic mean for the vdW radii is preferable. The related formula can be used for reasonable estimations of the equilibrium distance providing the relative error within 10%. However, Eq. (9), as the generalization of Eq. (7), provides much more accurate results with R.E. within 2.5%, $\langle \text{R.E.} \rangle = 0.2\%$ and $\langle |\text{R.E.}| \rangle = 1\%$.

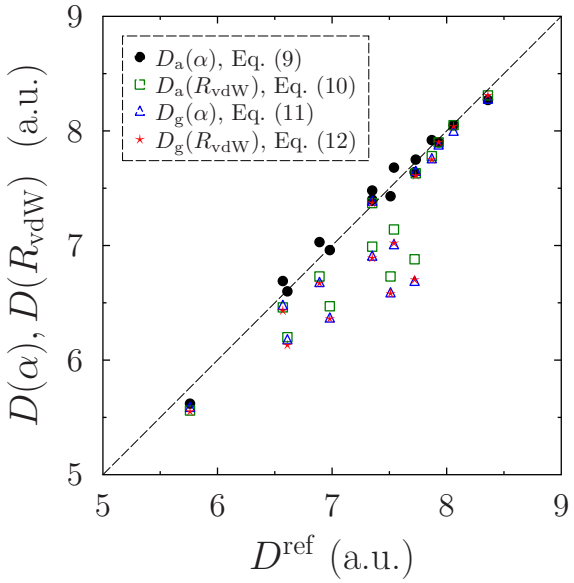

FIG. S 2: (Color online) The equilibrium distance of 15 vdW-bonded heteronuclear dimers of the noble gases (all possible pairs between He, Ne, Ar, Kr, Xe, and Rn) calculated with Eqs. (9)–(12) versus its reference counterpart [31].

Calculation of the effective atomic vdW radius in molecules

Here, we present detailed numerical results of our test calculations performed for molecular dimers from the S66 database [47] by means of the Tkatchenko-Scheffler (TS) method [10] with the Perdew-Burke-Ernzerhof (PBE) exchange-correlation functional [37]. The absolute and relative error of the interaction energy with respect to the coupled-cluster reference data [48] are obtained either with the old

$$R_{\rm vdW}^{\rm eff} = \left(\alpha^{\rm eff}/\alpha^{\rm free}\right)^{1/3} R_{\rm vdW}^{\rm free} = \left(V^{\rm eff}/V^{\rm free}\right)^{1/3} R_{\rm vdW}^{\rm free} \tag{S18}$$

or new

$$R_{\rm vdW}^{\rm eff} = 2.54 \left(\alpha^{\rm eff}\right)^{1/7} \tag{S19}$$

way to calculate the effective atomic vdW radius in molecules. Here, the polarizability/volume ratio is obtained by means of the Hirshfeld partitioning of the electron density [10].

Similar to the approach of Ref. [10], we refitted the TS damping parameter s_R employing Eq. (S19) on the S22 benchmark set of molecular dimers [38]. With its new value of 0.91, in comparison to 0.94 [10] obtained with the old scheme based on Eq. (S18), we perform our test calculations on the S66 dataset [47,48]. The corresponding density-functional calculations have been carried out using the all-electron code FHI-aims [39] with *tight* defaults.

As demonstrated by Table S IV, the new approach provides better accuracy for 57 from 66 molecular dimers. For nine other systems, the difference between the absolute errors related to the two approaches is still much less than the chemical accuracy (1 kcal/mol). Therefore, we may conclude that Eq. (S19) provides a general improvement of the used procedure. The mean relative error and its magnitude change from -11.5% to -7.4% and from 12.0% to 8.8%, respectively, by using the new approach instead of the old one. That corresponds to the accuracy improvement by about 30%.

This finding provides an additional confirmation of the revealed scaling law pointing out to a quite non-trivial quantum-mechanical relation between the atomic volume and the vdW radius.

Symmetry-adapted perturbation theory analysis

With the symmetry-adapted perturbation theory (SAPT) decomposition, one obtains six contributions: electrostatic ($E_{\rm pol}^{(1)}$), exchange ($E_{\rm exch}^{(1)}$), induction ($E_{\rm ind}^{(2)}$), exchange-induction ($E_{\rm exch-ind}^{(2)}$), dispersion ($E_{\rm disp}^{(2)}$), and exchange-dispersion ($E_{\rm exch-disp}^{(2)}$). In the case of neutral systems, the net in-

duction interaction ($E^{(2)}_{\rm ind}+E^{(2)}_{\rm exch-ind}$) is almost zero due to the balance between its constituents [40] and the decomposition can be restricted to the four other contributions. For noble gas dimers, numerical results of the SAPT based on coupled-cluster approach with single and double excitations (CCSD) were provided recently in Ref. [41]. The authors have shown that their calculations are in good agreement with corresponding density-functional theory (DFT) based SAPT approaches. By using their data, we evaluate the SAPT contributions to attractive and repulsive forces for He-He, Ne-Ne, Ar-Ar, and Kr-Kr dimers considered in Ref. [41]. The magnitude of corresponding contributions is obtained within the following spans: $0.15 < F^{(1)}_{\rm pol}/F^{(1)}_{\rm exch} < 0.35$, $0.65 < F^{(2)}_{\rm disp}/F^{(1)}_{\rm exch} < 0.82$, and $0.05 < F^{(2)}_{\rm exch-disp}/F^{(1)}_{\rm exch} < 0.13$, where the maximal contribution $F^{(1)}_{\rm exch}$ is chosen as a reference. The net induction force ($F^{(2)}_{\rm ind} + F^{(2)}_{\rm exch-ind}$) is one order of magnitude less than $F^{(2)}_{\rm exch-disp}$ and therefore can be disregarded. This analysis shows that the force stemming from the electrostatic interaction has a relevant contribution. However, by its definition (for instance, Eq. (1) in Ref. [42]), $E^{(1)}_{\rm pol}$ is equal to the Coulomb integral which, like our Eq. (S4), vanishes in the dipole approximation for spherically symmetric atomic electron densities. Therefore, the corresponding force can contribute only for higher-order terms in multipole expansion of the Coulomb potential. Its influence needs to be considered for derivation of the general relationship given by Eq. (13), but it is irrelevant for our derivation of the scaling law expressed by Eq. (7).

---

[34] K. T. Tang and J. P. Toennies, *An improved simple model for the van der Waals potential based on universal damping functions for the dispersion coefficients*, J. Chem. Phys. **80**, 3726 (1984).

[35] L. M. Wei, P. Li, and K. T. Tang, *Iterative combining rules for the van der Waals potentials of mixed rare gas systems*, Chem. Phys. Lett. **675**, 40 (2017).

[36] K. T. Tang, J. P. Toennies, M. Wanschura, and C. L. Yiu, *Exchange energy of alkali-metal dimer cations calculated from the atomic polarizability with the Holstein-Herring method*, Phys. Rev. A **46**, 3746 (1992).

[37] J. P. Perdew, K. Burke, and M. Ernzerhof, *Generalized gradient approximation made simple*, Phys. Rev. Lett. **77**, 3865 (1996).

[38] P. Jurecka, J. Sponer, J. Cerny, and P. Hobza, *Benchmark database of accurate (MP2 and CCSD(T) complete basis set limit) interaction energies of small model complexes, DNA base pairs, and amino acid pairs*, Phys. Chem. Chem. Phys. **8**, 1985 (2006).

[39] V. Blum, R. Gehrke, F. Hanke, P. Havu, V. Havu, X. Ren, K. Reuter, and M. Scheffler, *Ab initio molecular simulations with numeric atom-centered orbitals*, Comput. Phys. Commun. **180**, 2175 (2009).

[40] A. Heßelmann and T. Korona, *Intermolecular symmetry-adapted perturbation theory study of large organic complexes*, J. Chem. Phys. **141**, 094107 (2014).

[41] L. Shirkov and V. Sladek, *Benchmark CCSD-SAPT study of rare gas dimers with comparison to MP-SAPT and DFT-SAPT*, J. Chem. Phys. **147**, 174103 (2017).

[42] A. Heßelmann, G. Jansen, and M. Schütz, *Density-functional theory-symmetry-adapted intermolecular perturbation theory with density fitting: A new efficient method to study intermolecular interaction energies*, J. Chem. Phys. **122**, 014103 (2005).

TABLE SII: The van der Waals radius calculated according to Eq. (7) with the atomic dipole polarizability taken either from Ref. [12] ($\alpha^{(1)}$) or from Ref. [14] ($\alpha^{(2)}$) is presented in comparison to its reference [15] counterpart. The relative error (R.E.) is calculated by Eq. (8). A comment: for Th and U, there are no data in Ref. [14].

Species	$R_{\rm vdW}^{\rm ref}$	$\alpha^{(1)}$	$R_{\rm vdW}(\alpha^{(1)})$	R.E.	$\alpha^{(2)}$	$R_{\rm vdW}(\alpha^{(2)})$	R.E.
Li	4.9700	164.2000	5.2640	+5.92%	164.00	5.2631	+5.90%
Be	4.2141	38.0000	4.2709	+1.35%	37.70	4.2660	+1.23%
B	3.8739	21.0000	3.9239	+1.29%	20.50	3.9105	+0.94%
C	3.7039	12.0000	3.6225	−2.20%	11.70	3.6094	−2.55%
N	3.3826	7.4000	3.3807	−0.06%	7.25	3.3709	−0.35%
O	3.2314	5.4000	3.2319	+0.02%	5.20	3.2146	−0.52%
F	3.1180	3.8000	3.0737	−1.42%	3.60	3.0500	−2.18%
Na	5.2345	162.7000	5.2571	+0.43%	163.00	5.2585	+0.46%
Mg	4.5731	71.0000	4.6698	+2.11%	71.40	4.6736	+2.20%
Al	4.5353	60.0000	4.5589	+0.52%	57.50	4.5312	−0.09%
Si	4.2708	37.0000	4.2546	−0.38%	37.00	4.2546	−0.38%
P	4.0440	25.0000	4.0229	−0.52%	24.80	4.0183	−0.64%
S	3.8928	19.6000	3.8855	−0.19%	19.50	3.8826	−0.26%
Cl	3.8739	15.0000	3.7398	−3.46%	14.70	3.7290	−3.74%
K	5.7070	292.9000	5.7177	+0.19%	290.00	5.7096	+0.05%
Ca	5.2534	160.0000	5.2446	−0.17%	160.00	5.2446	−0.17%
Sc	4.9511	120.0000	5.0334	+1.66%	123.00	5.0512	+2.02%
Ti	4.6109	98.0000	4.8898	+6.05%	102.00	4.9179	+6.66%
V	4.2897	84.0000	4.7833	+11.51%	87.30	4.8098	+12.12%
Cr	4.2141	78.0000	4.7330	+12.31%	78.40	4.7364	+12.40%
Mn	4.2519	63.0000	4.5907	+7.97%	66.80	4.6293	+8.88%
Fe	4.2897	56.0000	4.5141	+5.23%	60.40	4.5632	+6.38%
Co	4.2519	50.0000	4.4416	+4.46%	53.90	4.4896	+5.59%
Ni	4.2141	48.0000	4.4158	+4.79%	48.40	4.4211	+4.91%
Cu	4.2897	42.0000	4.3324	+1.00%	41.70	4.3280	+0.89%
Zn	4.2330	40.0000	4.3023	+1.64%	38.40	4.2773	+1.05%
Ga	4.5542	60.0000	4.5589	+0.10%	52.10	4.4678	−1.90%
Ge	4.3842	41.0000	4.3175	−1.52%	40.20	4.3054	−1.80%
As	4.2519	29.0000	4.1091	−3.36%	29.60	4.1212	−3.08%
Se	4.1196	25.0000	4.0229	−2.35%	26.20	4.0499	−1.69%
Br	3.9684	20.0000	3.8967	−1.81%	21.60	3.9398	−0.72%
Rb	5.9526	319.2000	5.7884	−2.76%	317.00	5.7827	−2.86%
Sr	5.5558	199.0000	5.4106	−2.61%	198.00	5.4067	−2.68%
Y	5.1212	126.7370	5.0728	−0.94%	163.00	5.2585	+2.68%
Zr	4.8566	119.9700	5.0332	+3.64%	112.00	4.9840	+2.62%
Nb	4.6487	101.6030	4.9151	+5.73%	97.90	4.8891	+5.17%
Mo	4.5164	88.4225	4.8185	+6.69%	87.10	4.8082	+6.46%
Tc	4.4787	80.0830	4.7508	+6.08%	79.60	4.7467	+5.99%
Ru	4.4787	65.8950	4.6203	+3.16%	72.30	4.6819	+4.54%
Rh	4.3842	56.1000	4.5153	+2.99%	66.40	4.6253	+5.50%
Pd	4.4409	23.6800	3.9919	−10.11%	61.70	4.5771	+3.07%

Species	$R_{\mathrm{vdW}}^{\mathrm{ref}}$	$\alpha^{(1)}$	$R_{\mathrm{vdW}}(\alpha^{(1)})$	R.E.	$\alpha^{(2)}$	$R_{\mathrm{vdW}}(\alpha^{(2)})$	R.E.
Ag	4.4787	50.6000	4.4492	−0.66%	46.20	4.3918	−1.94%
Cd	4.4787	39.7000	4.2977	−4.04%	46.70	4.3985	−1.79%
In	4.7810	70.2200	4.6625	−2.48%	62.10	4.5813	−4.18%
Sn	4.6487	55.9500	4.5136	−2.91%	60.00	4.5589	−1.93%
Sb	4.5542	43.6719	4.3566	−4.34%	44.00	4.3613	−4.24%
Te	4.4598	37.6500	4.2652	−4.36%	40.00	4.3023	−3.53%
I	4.1952	35.0000	4.2210	+0.62%	33.60	4.1965	+0.03%
Cs	6.2361	427.1200	6.0343	−3.24%	396.00	5.9694	−4.28%
Ba	5.7637	275.0000	5.6664	−1.69%	278.00	5.6752	−1.53%
La	5.3101	213.7000	5.4659	+2.93%	214.00	5.4670	+2.95%
Hf	4.7621	99.5200	4.9006	+2.91%	83.70	4.7809	+0.39%
Ta	4.5731	82.5300	4.7713	+4.33%	73.90	4.6966	+2.70%
W	4.4598	71.0410	4.6702	+4.72%	65.80	4.6193	+3.58%
Re	4.4409	63.0400	4.5912	+3.38%	60.20	4.5610	+2.71%
Os	4.4031	55.0550	4.5032	+2.27%	55.30	4.5060	+2.34%
Ir	4.4220	42.5100	4.3399	−1.86%	51.30	4.4580	+0.81%
Pt	4.4787	39.6800	4.2974	−4.05%	48.00	4.4158	−1.40%
Au	4.5542	36.5000	4.2464	−6.76%	45.40	4.3808	−3.81%
Hg	4.2519	33.9000	4.2018	−1.18%	33.50	4.1947	−1.35%
Tl	4.7810	69.9200	4.6596	−2.54%	51.40	4.4592	−6.73%
Pb	4.7810	61.8000	4.5781	−4.24%	47.90	4.4145	−7.67%
Bi	4.7621	49.0200	4.4291	−6.99%	43.20	4.3499	−8.66%
Th	5.1967	217.0000	5.4779	+5.41%	—	—	—
U	5.0078	127.8000	5.0789	+1.42%	—	—	—

TABLE S III: The equilibrium distance of 15 vdW-bonded heteronuclear dimers of the noble gases (all possible pairs between He, Ne, Ar, Kr, Xe, and Rn) calculated with Eqs. (9)–(12) in comparison to the reference values [31].

Dimer	D^{ref}	$D_{\mathrm{a}}(\alpha)$	R.E.	$D_{\mathrm{a}}(R_{\mathrm{vdW}})$	R.E.	$D_{\mathrm{g}}(\alpha)$	R.E.	$D_{\mathrm{g}}(R_{\mathrm{vdW}})$	R.E.
He-Ne	5.76	5.62	−2.43%	5.56	−3.47%	5.58	−3.13%	5.55	−3.58%
He-Ar	6.61	6.60	−0.15%	6.20	−6.20%	6.17	−6.66%	6.13	−7.20%
He-Kr	6.98	6.96	−0.29%	6.47	−7.31%	6.36	−8.88%	6.36	−8.83%
He-Xe	7.51	7.43	−1.07%	6.73	−10.39%	6.58	−12.38%	6.58	−12.43%
He-Rn	7.72	7.64	−1.04%	6.88	−10.88%	6.68	−13.47%	6.70	−13.26%
Ne-Ar	6.57	6.69	+1.83%	6.46	−1.67%	6.47	−1.52%	6.43	−2.16%
Ne-Kr	6.89	7.03	+2.03%	6.73	−2.32%	6.67	−3.19%	6.67	−3.22%
Ne-Xe	7.35	7.48	+1.77%	6.99	−4.90%	6.90	−6.12%	6.89	−6.24%
Ne-Rn	7.54	7.68	+1.86%	7.14	−5.31%	7.00	−7.16%	7.02	−6.94%
Ar-Kr	7.35	7.40	+0.68%	7.37	+0.27%	7.38	+0.41%	7.37	+0.20%
Ar-Xe	7.73	7.75	+0.26%	7.63	−1.29%	7.64	−1.16%	7.61	−1.53%
Ar-Rn	7.87	7.92	+0.64%	7.78	−1.14%	7.75	−1.52%	7.75	−1.52%
Kr-Xe	7.93	7.90	−0.38%	7.90	−0.38%	7.87	−0.76%	7.90	−0.43%
Kr-Rn	8.06	8.05	−0.12%	8.05	−0.12%	7.99	−0.87%	8.04	−0.25%
Xe-Rn	8.36	8.27	−1.08%	8.31	−0.60%	8.27	−1.08%	8.31	−0.61%

TABLE SIV: Absolute (A.E. in kcal/mol) and relative (R.E.) error for the interaction energy of molecular dimers from the S66 database [47,48] obtained either with the old or new scaling law.

SYSTEM NAME	A.E. (OLD)	R.E. (OLD)	A.E. (NEW)	R.E. (NEW)	|A.E. (OLD)| − |A.E. (NEW)|
WaterWater	−0.35	−7.1%	−0.30	−6.1%	+0.05
WaterMeOH	−0.26	−4.6%	−0.16	−2.8%	+0.10
WaterMeNH2	−0.96	−13.7%	−0.86	−12.3%	+0.10
WaterPeptide	−0.07	−0.8%	+0.06	+0.7%	+0.00
MeOHMeOH	−0.26	−4.5%	−0.18	−3.2%	+0.08
MeOHMeNH2	−1.06	−14.0%	−0.93	−12.2%	+0.13
MeOHPeptide	−0.33	−3.9%	−0.25	−3.0%	+0.08
MeOHWater	−0.31	−6.2%	−0.28	−5.5%	+0.04
MeNH2MeOH	−0.43	−13.8%	−0.34	−10.9%	+0.09
MeNH2MeNH2	−0.41	−9.7%	−0.21	−4.9%	+0.20
MeNH2Peptide	−0.09	−1.7%	+0.08	+1.5%	+0.01
MeNH2Water	−0.68	−9.2%	−0.53	−7.2%	+0.15
PeptideMeOH	−0.04	−0.7%	+0.10	+1.6%	−0.06
PeptideMeNH2	−0.71	−9.4%	−0.48	−6.4%	+0.23
PeptidePeptide	−0.24	−2.7%	−0.06	−0.7%	+0.18
PeptideWater	−0.03	−0.7%	+0.02	+0.4%	+0.02
UracilUracilBP	−0.19	−1.1%	−0.12	−0.7%	+0.07
WaterPyridine	−0.77	−11.1%	−0.68	−9.8%	+0.09
MeOHPyridine	−0.73	−9.8%	−0.65	−8.7%	+0.08
AcOHAcOH	−0.89	−4.6%	−0.82	−4.2%	+0.07
AcNH2AcNH2	−0.19	−1.2%	−0.09	−0.5%	+0.10
AcOHUracil	−0.42	−2.1%	−0.35	−1.8%	+0.07
AcNH2Uracil	−0.14	−0.7%	−0.05	−0.2%	+0.09
BenzeneBenzenepipi	−0.71	−25.7%	−0.64	−23.2%	+0.07
PyridinePyridinepipi	−0.70	−18.4%	−0.59	−15.3%	+0.12
UracilUracilpipi	+0.02	+0.2%	+0.23	+2.3%	−0.21
BenzenePyridinepipi	−0.73	−21.6%	−0.63	−18.7%	+0.10
BenzeneUracilpipi	−0.37	−6.6%	−0.19	−3.4%	+0.18
PyridineUracilpipi	−0.19	−2.8%	−0.02	−0.2%	+0.17
BenzeneEthene	−0.58	−41.6%	−0.52	−37.3%	+0.06
UracilEthene	−0.31	−9.2%	−0.13	−3.8%	+0.18
UracilEthyne	−0.07	−1.8%	+0.05	+1.3%	+0.02
PyridineEthene	−0.55	−30.2%	−0.45	−24.6%	+0.10
PentanePentane	−1.29	−34.5%	−0.86	−23.0%	+0.43
NeopentanePentane	−0.76	−29.1%	−0.54	−20.7%	+0.22
NeopentaneNeopentane	−0.66	−37.8%	−0.57	−32.7%	+0.09
CyclopentaneNeopentane	−0.95	−39.9%	−0.73	−30.5%	+0.22
CyclopentaneCyclopentane	−1.11	−37.1%	−0.80	−27.0%	+0.30
BenzeneCyclopentane	−0.80	−22.6%	−0.50	−14.2%	+0.30
BenzeneNeopentane	−0.49	−17.2%	−0.30	−10.5%	+0.19

SYSTEM NAME	A.E. (OLD)	R.E. (OLD)	A.E. (NEW)	R.E. (NEW)	|A.E. (OLD)| − |A.E. (NEW)|
UracilPentane	−0.55	−11.5%	−0.16	−3.3%	+0.40
UracilCyclopentane	−0.55	−13.4%	−0.23	−5.7%	+0.32
UracilNeopentane	−0.41	−11.1%	−0.15	−4.2%	+0.26
EthenePentane	−0.67	−33.5%	−0.36	−18.3%	+0.30
EthynePentane	−0.58	−33.5%	−0.49	−28.4%	+0.09
PeptidePentane	−0.73	−17.3%	−0.28	−6.6%	+0.45
BenzeneBenzeneTS	−0.05	−1.7%	+0.11	+4.0%	−0.07
PyridinePyridineTS	+0.04	+1.0%	+0.23	+6.5%	−0.19
BenzenePyridineTS	−0.02	−0.6%	+0.15	+4.4%	−0.12
BenzeneEthyneCHpi	−0.01	−0.3%	+0.11	+4.0%	−0.10
EthyneEthyneTS	−0.24	−15.5%	−0.19	−12.6%	+0.04
BenzeneAcOHOHpi	+0.10	+2.2%	+0.20	+4.3%	−0.10
BenzeneAcNH2NHpi	−0.07	−1.7%	+0.08	+1.8%	−0.01
BenzeneWaterOHpi	−0.34	−10.3%	−0.22	−6.7%	+0.12
BenzeneMeOHOHpi	−0.40	−9.6%	−0.25	−6.0%	+0.15
BenzeneMeNH2NHpi	−0.33	−10.2%	−0.18	−5.5%	+0.15
BenzenePeptideNHpi	−0.17	−3.3%	+0.01	+0.3%	+0.16
PyridinePyridineCHN	+0.45	+10.7%	+0.52	+12.3%	−0.07
EthyneWaterCHO	−0.14	−4.9%	−0.10	−3.4%	+0.04
EthyneAcOHOHpi	−0.24	−4.9%	−0.16	−3.3%	+0.08
PentaneAcOH	−0.73	−25.2%	−0.47	−16.4%	+0.25
PentaneAcNH2	−0.72	−20.4%	−0.44	−12.6%	+0.27
BenzeneAcOH	−0.34	−8.9%	−0.12	−3.1%	+0.22
PeptideEthene	−0.37	−12.2%	−0.13	−4.3%	+0.24
PyridineEthyne	−0.36	−9.0%	−0.29	−7.2%	+0.07
MeNH2Pyridine	−0.28	−7.0%	−0.09	−2.3%	+0.19